# Influence of niobium on stacking-fault energy of all-austenite stainless steels

Luis G. Martinez, Kengo Imakuma and Angelo F. Padilha

The effects of niobium addition on a completely austenitic stainless steel matrix consisting of Fe-15%Cr-15%Ni, with about 0, 0.5, 1 and 2% niobium, were studied by determination of stacking fault energies by means of X-ray diffraction analysis. A strong influence of niobium on stacking-fault energies was found, whose behaviour can be explained as being due to decrease in the electron/atom ratio and increase in the L. Pauling electron vacancy number of austenitic Fe-Cr-Ni matrix brought on by niobium.

**Einfluß von Niob auf die Stapelfehlerenergie von vollaustenitischen, nichtrostenden Stählen.** Mit Hilfe der Bestimmung von Stapelfehlerenergien durch eine Röntgendiffraktometer-Analyse wurde der Einfluß von Niobzusätzen (0, 0,5, 1 und 2%) auf die Matrix einer vollaustenitischen Fe-15%Cr-15%Ni-Legierung untersucht. Es wurde eine starke Abhängigkeit der Stapelfehlerenergie vom Niobgehalt festgestellt, was dadurch erklärt werden kann, daß durch den Niobzusatz in der austenitischen Fe-Cr-Ni-Matrix das Verhältnis Elektronen/Atome abgesenkt und die L.-Pauling-Elektronen-Leerstellenanzahl erhöht wurde.

The stacking-fault energy (SFE) is one of the most important parameters of metals and alloys since it is directly associated with numerous properties of such materials. For instance, the SFE of austenitic stainless steels is closely related to the density and distribution of crystal defects induced by plastic deformation (such as dislocations), to work-hardening rate, to creep behaviour, to fatigue behaviour, to stress-corrosion cracking, to irradiation void swelling, to deformation-induced martensite (mainly $\varepsilon$-hexagonal martensite) and to annealing twin frequency[1]). The SFE of a stainless steel is basically governed by the average electron/atom ratio or by the L. Pauling[2]) electron vacancy number of the austenite.

A number of methods has been proposed to measure the SFE. One of the experimental methods is by direct observation of dislocation nodes, loops or tetrahedra by transmission electron microscopy. The observation of extended dislocation node curvature radii in materials with SFE lower than 50 mJ/m$^2$ is considered to be very accurate. The indirect methods for SFE determination include the measurement of texture by X-ray, third stage single-crystal work-hardening rates and combined X-ray measurements of stacking-fault probability and rms microstrain[3]).

Niobium-stabilized stainless steels have been used in both normal and high-temperature service environments. The study of the effect of niobium on the microstructure and properties of austenitic stainless steels has traditionally been performed on alloys with considerably higher chromium content than nickel, which are not completely austenitic. The niobium in these steels is usually present in the form of carbides and it can also enhance the formation of $\delta$-ferrite and the precipitation of Laves phase $Fe_2Nb$[4])[5]).

The central idea of the present investigation is to study the effects of niobium additions on completely austenitic matrices. In order to do this a base matrix consisting of Fe-15%Cr-15%Ni was selected and about 0.5, 1 and 2% niobium added. The carbon content was kept very low to minimize the niobium consumption due to the NbC formation.

*M. Sc. Luis G. Martinez; Dr. Eng. Kengo Imakuma*, Institute of Energetic and Nuclear Research, National Commission of Nuclear Energy, IPEN-CNEN, São Paulo; *Professor Dr. Angelo F. Padilha*, Department of Metallurgical and Materials Engineering, University of São Paulo, Brazil.

## Preparation and microstructural characterization of the alloys

The alloys with different niobium content, as shown in table 1, were prepared by vacuum induction melting from high-purity materials. The resulting 20 kg ingots were reduced 95% by forging, between 1200 and 950 °C, followed by solution annealing.

The microstructure was analyzed by several complementary techniques. Microstructural characterization of the alloys in the as-cast, as-cast and solubilized, as-forged and as-forged and solubilized states consisted of macrographic analysis, magnetic tests to detect the presence of $\delta$-ferrite and $\alpha'$-martensite, optical microscopy and scanning electron microscopy with energy dispersive analysis. Precipitates were also isolated from the metallic matrix and the filtered residue analysed in a Debye-Scherrer diffraction camera.

Almost all the niobium present in the as-cast alloys was precipitated in the form of eutectic colonies of hexagonal Laves phase $(Fe,Cr,Ni)_2(Nb,Si)$ and a few particles of Nb(C,N). The Laves phase had lattice parameters $a_0$ = 0.476 nm and $c_0$ = 0.786 nm and the fcc carbonitride showed $a_0$ = 0.445 nm. All the alloys were found to be free from $\delta$-ferrite. Homogenization of the as-cast Nb-containing alloys at 1200 °C did not modify their mi-

**Table 1.** Chemical compositions (wt. %) of the investigated alloys

| Element | alloy A | B | C | D |
|---|---|---|---|---|
| Cr | 14.4 | 14.7 | 15.1 | 14.6 |
| Ni | 15.1 | 15.1 | 14.1 | 14.8 |
| C | 0.02 | 0.02 | 0.02 | 0.02 |
| Nb | <0.002 | 0.44 | 0.89 | 1.74 |
| Si | 0.59 | 0.48 | 0.53 | 0.57 |
| Mn | 0.53 | 0.43 | 0.52 | 0.47 |
| P | 0.006 | 0.006 | 0.006 | 0.006 |
| S | 0.013 | 0.012 | 0.012 | 0.012 |
| Cu | 0.02 | 0.04 | 0.01 | 0.01 |
| Al | <0.005 | <0.005 | <0.005 | <0.005 |
| Sn | 0.002 | 0.002 | 0.001 | 0.001 |
| As | 0.002 | 0.001 | 0.002 | 0.002 |
| N | 0.0084 | 0.0081 | 0.0071 | 0.0081 |
| Mo | 0.01 | 0.01 | <0.01 | <0.01 |

crostructures. The microstructure of the as-forged alloys consisted of recrystallized grains and fragmented Laves-phase particles. Most of the niobium was in solid solution after the forging and solution annealing processes. However, even 3 h treatment at 1270 °C was found to be insufficient for complete dissolution of the Laves phase in the alloy D. The maximum solid solubility of niobium in the Fe-15%Cr-15%Ni austenitic matrix was estimated to be 1.67 ± 0.11 wt. %[6]).

## SFE measurement procedure and results

The X-ray method for the determination of SFE employed in this work consisted in relating the SFE with the ratio $< \epsilon_{50}^2 >_{111} / \alpha$ expressed by the relation[3]):

$$\gamma = \frac{G_{111} K_{111} w_0 a_0}{\pi \sqrt{3}} \quad \frac{< \epsilon_{50}^2 >_{111}}{\alpha} \qquad (1)$$

where $\gamma$ is the SFE, $G_{111}$ is the shear modulus in the (111) fault plane, $K_{111}$ is a constant relating the dislocation density and stacking-fault probability, $w_0$ is a term related with elastic anisotropy, $a_0$ is the lattice parameter, $< \epsilon_{50}^2 >_{111}$ is the rms microstrain in the (111) direction averaged over a distance of 50 Å, and $\alpha$ the stacking-fault probability. The rms microstrain was determined by Fourier analysis of the broadening of X-ray diffraction profile by means of the Warren-Averbach's method and $\alpha$ was determined from the relative X-ray peak shifts[8]). The constant $K_{111} w_0$ was determined from the relationship between $\gamma$ and the measured ratio $< \epsilon_{50}^2 >_{111} / \alpha$ for pure metals and these values of SFE were extensively studied. The metals elected for this purpose were Ag, Au, Cu, Al and Ni. The values of SFE for these metals were compiled from two review articles[3])[7]), resulting in two different values of the constant $K_{111} w_0$[8]). From these values of SFE for pure metals reported by Reed and Schramm[3] and measured values of $< \epsilon_{50}^2 >_{111}$ and $\alpha$ for each metal, the value $K_{111} w_0 = 6.37$ was obtained, and using the values of SFE reported by Coulomb[7]), the value $K_{111} w_0 = 4.91$ was found. These values are consistent with the range of values obtained in similar works, as discussed by Martinez[8]). The lattice parameter of the alloys was experimentally determined as $a_0 = 3.586 \pm 0.005$ Å, and the shear modulus was inferred from reported values for similar alloys[9]).

**Table 2** shows the values of SFE for the alloys calculated using both the values of $K_{111} w_0 = 6.37$ (a) and $K_{111} w_0 = 4.91$ (b) and the average value (c).

## Discussion

Austenitic stainless steels, based on the iron-nickel-chromium system, have relatively low stacking-fault energies and consequently undergo quench and/or deformation-induced stacking-fault formation in the face centered cubic (fcc) austenitic matrix. In certain compositions the austenite may also transform to the hexagonal close-packed (hcp) $\epsilon$ and the body centered (bcc) $\alpha$'-martensite phases during quenching and/or cold deformation[10]). Most of the alloying elements in solution in austenitic steels reduce the $M_s(\alpha')$ and $M_d(\alpha')$ temperatures. $M_s(\epsilon)$ and $M_d(\epsilon)$ compositional relationship have not been derived for the $\epsilon$-martensite[11]). The formation of the $\epsilon$-phase appears to be strongly dependent on the stacking-fault energy[12]). The presence and quantity of $\alpha$' and $\epsilon$ phases are also dependent on the strain-rate as well as temperature, amount and mode of deformation.

**Table 2.** Stacking fault energies of the alloys; (a) using $K_{111} w_0 = 6.37$; (b) using $K_{111} w_0 = 4.91$; (c) average values

| Alloy | %Nb | SFE [mJ/m²] (a) | (b) | (c) |
|---|---|---|---|---|
| A | 0 | 53 | 38 | 46 |
| B | 0.44 | 32 | 23 | 28 |
| C | 0.89 | 27 | 19 | 23 |
| D | 1.74 | 25 | 18 | 22 |

The SFE of alloy A is almost twice that of the commonly reported values for AISI 304, 316, 321 and 347 stainless steels[9]). The high nickel content and low chromium content of the alloy A compared to steels of series 300 can explain such difference in SFE value. The high SFE for alloy A explains the presence of well defined dislocation cells observed by means of transmission electron microscopy in commercial steel (DIN 1.4970) of a similar matrix, as reported in a previous work[13]).

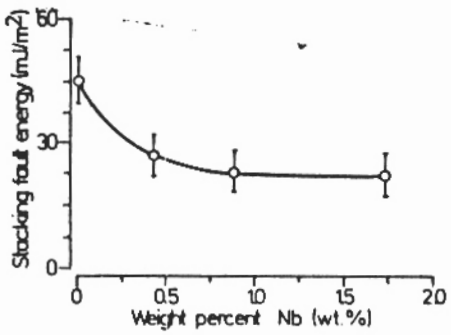


**Figure 1.** Stacking-fault energies (SFE) of the alloys vs. Nb content

The measured values of SFE for alloys B, C and D show a strong influence of niobium on stacking-fault energies, as evidenced by the results in **figure 1**. This behaviour can be explained as being due to decrease in the electron/atom ratio and increase in the mean electron vacancy number of austenitic Fe-Cr-Ni brought on by niobium. Each Nb atom contributes with only 5 electrons to the electron/atom ratio, while iron, chromium and nickel contribute with 8, 6 and 8, respectively. The average electron vacancy number ($\bar{EVN}$) of matrix is given by[1]):

$$(\bar{EVN}) = 0.61[\%Ni] + 2.66[\%Fe] + 3.66[\%Mn] + 4.66[\%Cr] + 5.66[\%Nb] + 6.66[\%Si] \qquad (2)$$

where the concentrations of the components in solid solution (wt.%) appear in the brackets.

## Conclusion

The niobium strongly decreases the stacking-fault energy of 15%Cr-15%Ni austenite, as shown in figure 1. This de-

crease of SFE was not enough to cause the occurrence of strain-induced martensites.

(A00677, received: 13. February 1992)

## References


[1]) *Borges, J. F. A.; Padilha, A. F.; Imakuma, K.:* Revista de Física Aplicada e Instrumentação, Brazil 1 (1986), p. 335/51.
[2]) *Pauling, L.:* Phys. Rev. 54 (1938), p. 899/905.
[3]) *Reed, R.P., Schramm, R. E.:* J. Appl. Phy. 45 (1974), p. 4705/11.
[4]) *Pigatin, W. L., Bueno, L. O.:* Metalurgia - ABM, Brazil 46 (1990), p. 1989.
[5]) *Kestenbach, H. J., Bueno, L. O.:* Mat. Sci. Eng. 66 (1984), p. L19/23.
[6]) *Padilha, A. F.:* Efeito do nióbio na microestrutura e nas propriedades da austenita inoxidável Fe-Cr-Ni. Theses Livre Docência, Universidade de São Paulo, Brazil, 1989.
[7]) *Coulomb, P.:* J. Microsc. Spect. Eletr. 3 (1978), p. 295/301.
[8]) *Martinez, L. G.:* Determinação da energia de defeito de empilhamento por difração de Raios-X. Master Thesis, IPEN - Universidade de São Paulo, Brazil, 1989.
[9]) *Schramm, R. E.; Reed, R. P.:* Met. Trans. 6 A (1975), p. 1345/51.
[10]) *Bowkett, M. W.; Keown, S. R.; Harries, D. R.:* Met. Sci. 16 (1982), p. 499/517.
[11]) *Harries, D. R.:* Proc. Int. Conf. Mech. Behaviour and Nuclear Applications of Stainless Steels at Elevated Temperatures, Varese, May 1981.
[12]) *Bowkett, M. W., Harries, D. R.:* AERE Report R-9093, April, 1978.
[13]) *Padilha, A. F.; Schanz, G.; Anderko, K.:* J. Nucl. Mat. 105 (1982), p. 77/92.


# ECSC announcements

## New contracts

Scientific and technical publications in the field of steel research published by the European Community Commission. The European Community Commission has announced the publication of the following final reports of ECSC research projects. The reports are obtainable from the European Community Bureau for Official Reports, P.O. Box 1003, L-2985 Luxemburg.
DE = German; EN = English; FR = French; IT = Italian; NL = Dutch; MF = report available on microfilm

### Materials technology

### Fatigue behaviour of butt-welded beam joints – Final report

*Becker, F.; Henrion, R.; Stammet, L.; Mang, F.; Bucak, O.*

*Arbed Recherches, Esch-sur-Alzhette (LU)*
*Contract No.: 7210-KD/501*
*EUR 13077 DE (1991), 238 pp., FS, ECU 20*
*ISBN 92-826-1945-1 (2)*

In contrast to welded built-up shapes, fatigue behaviour of butt-welded rolled beams has not been thoroughly investigated until now. As a consequence, several construction codes impose undue restrictions on the application of butt-welded rolled beams in the case of dynamic loads.

In order to correct this situation Arbed, in collaboration with the University of Karlsruhe (FRG), initiated fatigue tests on 74 full-scale samples of HE-300-B and HE-400-M beams, as well as on 44 small size samples, worked out of butt-welded beams. The influence on fatigue behavior of joint shape and welding conditions (shop or site welding), as well as the optimisation of joint preparation were investigated.

The results demonstrate significantly better fatigue behaviour in butt-welded joints of rolled beams than in built-up shapes. Joints prepared without windows at the webflange junction show an improved fatigue behaviour as compared to joints with windows. The present results should be taken into account in a new classification of butt-welded rolled beams in Eurocode 3. (AE 0332)

### HIC-resistant steel - structure and composite effects - Final report

*Dewsnap, R. F.*

*British Steel plc, London (GB)*
*Contract No.: 7210-KE/813*
*EUR 12959 EN (1990), 159 pp., FS, ECU 13.75*
*ISBN 92-826-1903-6 (2)*

The principal objective of this project was to assess the HIC resistance of a range of controlled rolled ultralow carbon enhanced alloy content AF/bainitic steels, compared with traditional ferrite-pearlite materials.

The various stages of the project are described, including the development of a suitable laboratory slab casting technique giving reproducible centreline segregation, the processing of a number of alloys to strength levels within the range X65-X80, HIC assessment and hydrogen permeation studies, and examination of segregation profiles in relation to compositional variables and HIC development. Finally, the results of a limited HIC assessment of laboratory simulated linepipe seam welds on the ultralow carbon AF/bainite and ferrite-pearlite steels is described. (AE 0313)

### The use of creep damage measurements in combination with material models for residual lifetime assesment

*Stamm, H.; von Estorff, U.*

*JRC Ispra (IT)*
*Paper presented: 8th European Conference on Fracture - ECF8, Torino (IT), Oct. 1–5, 1990*
*Available as Paper EN 35520 ORA*

Creep damage in an austenitic steel due to microcrack formation on grain boundary facets is considered. The metallographic examination is compared with non-destructive ultrasonic (US) velocity measurements. It is shown that both measurements can be related to a crack density parameter which also appears in the constitutive law for the creep strain rate. (AE 0310)